

# Defect-pool model and the hydrogen density of states in hydrogenated amorphous silicon

M. J. Powell and S. C. Deane

*Philips Research Laboratories, Redhill, Surrey, RH1 5HA, United Kingdom*

(Received 12 June 1995)

We present a treatment of the defect-pool model, for the calculation of the density of electronic gap states in hydrogenated amorphous silicon, based on the equilibration of *elemental* chemical reactions involving the separate release and capture of hydrogen. We derive the corresponding hydrogen density of states, describing the distribution of hydrogen binding energies, and show that the two densities of states are completely consistent. Hydrogen can be captured into weak SiSi bonds, which can be occupied by one or two hydrogen atoms. These are the dominant chemical reactions controlling the defect density. The effective hydrogen correlation energy is variable, being negative for most sites but positive where most defects occur. We show that the electronic density of states reproduces the main features of our earlier defect-pool model, with more charged defects than neutral defects for intrinsic amorphous silicon. The electronic density of states and the corresponding hydrogen density of states are consistent with a wide range of experimental results, including hydrogenation-dehydrogenation and hydrogen diffusion.

## I. INTRODUCTION

The density of electronic gap states in amorphous silicon is of fundamental importance. It is the key to understanding the basic physics of the material and it controls the performance of all device applications. The density of gap states can be divided into tail states originating from SiSi weak-bond states and defect states originating from Si dangling bonds. There is now widespread agreement that the density of Si dangling-bond states is determined by a chemical equilibrium process due to the interconversion of weak bonds and dangling bonds.<sup>1-4</sup>

If the energy of the dangling-bond state can take a range of values due to the inherent disorder of the amorphous network, then a proper consideration of the chemical equilibrium model, allowing for the formation of defects in different charge states, leads to densities of states with bands of positive, neutral, and negatively charged defects at different energies. This is the so-called *defect-pool* model.<sup>5,6</sup> Furthermore, allowing for the *simultaneous* formation of defects in all three charge states leads to significantly more charged than neutral defects in intrinsic amorphous silicon.<sup>5,7,8</sup>

The involvement of hydrogen in the equilibration process has been proposed following a wide range of experimental studies of the similarities between hydrogen diffusion and defect equilibration.<sup>9-12</sup> Hydrogen is not necessary for the basic defect-pool model, but it is found to be essential, not only in providing microscopic mechanisms for defect equilibration,<sup>13,14</sup> but equally in providing the necessary extra entropy from hydrogen reactions to give the observed defect densities.<sup>3,8</sup> No other mechanism has been proposed to date that can do this, to our knowledge.

The concept of the hydrogen density of states was introduced by Street<sup>15,16</sup> to represent the different binding energies of hydrogen atoms at different sites in the *a*-Si:H network. Originally the concept was applied to the growth surface, but later it was applied to the solid bulk phase. The energies of chemical reactions involving hydrogen motion were then represented by transitions on the hydrogen density

of states. The energy of the chemical reaction can also be represented as an electronic energy change and so there is a relationship between transitions on the hydrogen density of states and transitions on the electronic density of states.<sup>17</sup> Hydrogen motion, needed for complete equilibration, is then represented by the emission of hydrogen to a mobile interstitial, transport, and subsequent trapping in a SiSi or at a SiH site.

In this paper, we solve the defect-pool model, specifically for these chemical reactions, involving the separate emission and trapping of hydrogen. We show that the trapping of one or two hydrogen atoms in weak SiSi bonds is the dominant chemical reaction involving defects and that defects formed from the emission of hydrogen from isolated SiH bonds are negligible. We calculate the energy dependence of electronic states in the gap and the corresponding hydrogen density of states. In the defect-pool model, silicon dangling-bond states form with a distribution in energy and with different charge states. Hydrogen transitions involve silicon dangling-bond defects and so these transition energies will, in turn, depend on the defect energy and the Fermi energy. The hydrogen density of states thus becomes quite complex. In practice, the hydrogen density of states is dominated by the exponentially distributed weak-bond states and the underlying complexity is hidden.<sup>18</sup>

## II. THEORETICAL FRAMEWORK

### A. Chemical equations

Street and Winer<sup>3</sup> considered the following reactions for defect equilibration:



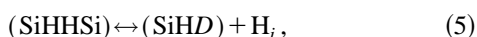
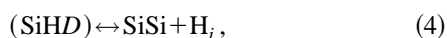
In reaction (1), hydrogen from an isolated SiH bond is inserted into a SiSi bond. Two defects are formed, which are chemically distinct. The *D* defect (denoted  $D_{\text{H}}$  by Street and

Winer) originates from the isolated SiH bond, while (SiHD) represents a singly hydrogenated SiSi bond, equivalent to an intimate, nonseparable, SiH bond and  $D$  defect (denoted  $D_w$  by Street and Winer). In reaction (2) a second hydrogen from another isolated SiH bond is inserted into the SiSi bond, forming a doubly hydrogenated bond denoted SiHHSi. Note that, according to reaction (2), SiSi bonds can have only zero or two hydrogen atoms, which means that the correlation energy for hydrogen occupancy is negative.<sup>13</sup> This is necessary to account for the fact that as  $a$ -Si:H is dehydrogenated and hydrogenated, orders of magnitude more hydrogen is removed than dangling bonds created.<sup>13</sup> The  $H_2^*$  complex proposed by Jackson<sup>14,19</sup> is one specific proposal for SiHHSi. In some papers, SiHHSi is referred to as SiHSiH to reflect the more likely spatial arrangement of the atoms, as in the  $H_2^*$  complex (where one hydrogen is on the bond-centered site and one on the  $T_d$  site). In  $a$ -Si:H there exists a range of bond angle and length disorder. This allows some relaxation and strain redistribution of the surrounding silicon atoms, resulting in a range of possible final configurations.<sup>19</sup> In this paper, we label this distribution of possibilities SiHHSi, to be consistent with our previous papers. This assignment makes no specific claim about the arrangement of the two H atoms, except that if they are both removed, then a SiSi bond reforms.

The equilibrium defect density can be solved by applying the law of mass action to the above reactions. When we include a distribution of SiSi (weak-bond) energies  $E_i$  and a range of defect energies  $E$  then this needs to be done differentially, allowing for equilibrium between weak bonds in a slice of energy  $dE_i$  and defects in a slice of energy  $dE$ . Care is needed in the application of the law of mass action, since different assumptions effectively correspond to different microscopic models and the appropriate model needs to be correctly applied.

The law of mass action is most appropriate for gas and liquid phase reactions, where all reactants are free to diffuse throughout the medium and react with all other reactants. In the solid phase, positions in the lattice are constrained, but the law of mass action can still be applied, providing not more than one component on each side of a multicomponent system reaction is immobile, thus allowing equilibration. Strictly speaking, applying the law of mass action to Eqs. (1) and (2) implies that SiH is mobile. In fact, SiH as a species is not mobile. Rather, we believe it is hydrogen that is mobile and so a more correct approach is to divide the defect creating reactions into elemental chemical reactions involving only truly mobile species, such as interstitial hydrogen and electrons. Thus the microscopic model becomes the release of hydrogen at one site, creating a dangling bond, followed by hydrogen diffusion through interstitial sites and capture into a SiSi weak-bond site, creating a second defect.

The elemental chemical equations that we need to solve are

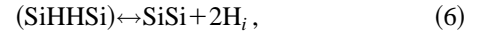


where  $H_i$  represents a mobile interstitial hydrogen atom. These equations should be solved independently, for a given concentration of  $H_i$ , by applying the law of mass action to each equation in turn. The microscopic details of hydrogen interstitial diffusion are not fully known. Here for simplicity we use a notation implying a single hydrogen mobility level, and a neutral mobile species. In fact, we shall later rewrite these equations in terms of the hydrogen chemical potential,  $\mu_H$ , and only solve equations where the details of the mobile hydrogen are eliminated. Thus, our work is quite general, and it would not matter what microscopic migration path the hydrogen takes, or even if the mobile hydrogen species was charged. This is analogous to the fact that, at equilibrium, dangling-bond *electron* occupancy depends only on the Fermi level (i.e., electron chemical potential), and not on the position or nature of the conduction-band mobility edge.

We can see that Eqs. (1) and (2) can be simply expressed as (3)–(4) and (3)+(3)–(4)–(5), respectively. However, applying the law of mass action to the elemental chemical reactions leads to *different* results from (1) and (2), when both the weak bonds and the defects have a distribution in energy. Physically this originates from the fact that the two defects are really formed independently and will minimize their free energy independently. In reactions (1) and (2) defects are formed locally in pairs and will minimize their free energy in pairs. However, even in the case where the defects *are* initially formed in pairs, say due to weak bond breaking, and then diffuse apart, the appropriate model is equivalent to the use of the elemental chemical reactions (3)–(5) and *not* (1) and (2). In a true chemical equilibrium, only the end points matter and not the intermediate reactions. Our model corresponds to a global equilibration between weak bonds and defects and the end point is two spatially and energetically independent defects.

## B. Key assumption

An important experimental observation is that device grade  $a$ -Si:H is very little affected by further hydrogenation or limited dehydrogenation.<sup>20,21</sup> No change is seen in the tail state distribution or in the defect density. The density of tail states is typically  $10^{20} \text{ cm}^{-3}$  and vastly more H atoms ( $3 \times 10^{21} \text{ cm}^{-3}$ ) are added or removed, without affecting the tail state distribution. This is an important observation and from this Nickel and Jackson<sup>20,21</sup> deduced that a combination of reactions (4) and (5) produce the chemical reaction



which must be *independent* of the SiSi bond energy. If during hydrogenation, H occupied only the weakest bonds, i.e., tail states, then a sharp reduction of the tail state density would occur on low-level hydrogenation. However, experiment shows that this does not occur. This means that reaction (6) must relate to a typical SiSi bond rather than a weak bond as was more commonly thought. The Si network can be hydrogenated or dehydrogenated over surprisingly wide limits without affecting the tail state or defect density. This places severe constraints on the possible models for hydrogen bonding in  $a$ -Si:H.

If we were to calculate the energy of reaction (6), by using the simple one-electron energies of the electron states,

TABLE I. Key reaction energies.

Chemical equations	H energy	Electron energy
(3) $\text{SiH} \leftrightarrow \text{D} + \text{H}_i$	$H_M - H_{\text{SiH}}$	$E + E_{\text{H}_i} - 2E_{\text{SiH}}$
(4) $\text{SiHD} \leftrightarrow \text{SiSi} + \text{H}_i$	$H_M - H^{0/1}$	$2E_i + E_{\text{H}_i} - 2E_{\text{SiH}} - E$
(5) $\text{SiHHSi} \leftrightarrow \text{SiHD} + \text{H}_i$	$H_M - H^{1/2}$	$E + E_{\text{H}_i} - 2E_{\text{SiH}} + 2(E_v - E_i)$
(6) $\text{SiHHSi} \leftrightarrow \text{SiSi} + 2\text{H}_i$	$2H_M - 2H_{\text{av}}$	$2E_{\text{H}_i} + 2E_v - 4E_{\text{SiH}}$

assuming the SiSi state is a tail state, then the right-hand side would contain the weak-bond energy  $E_i$ . This would result in weak bonds being preferentially occupied by hydrogen, inconsistent with the above experimental results. In order for reaction (6) *not* to depend on  $E_i$ , the left-hand side of Eq. (6) must contain an additional term than just the one-electron energy differences. One way of visualizing this is to recognize that the left-hand side can contain an additional strain term. The SiHHSi state creates strain in the surrounding silicon lattice, due to the fact it requires more space to accommodate the two H atoms in a SiSi bond compared to the unhydrogenated SiSi bond.<sup>19</sup> The strain energy is really a multielectronic term comprising distortion terms over the lattice surrounding the occupied SiSi bond. The net result is that other bonds are weakened, maintaining the distribution of weak bonds. If a doubly occupied bond state were to produce less strain energy than the energy of the bond state, then that bond would already be occupied with hydrogen. Thus the shape of the valence-band tail results from a steady-state situation during the hydrogenation of SiSi bonds. If a sample has no hydrogen, then the tail state distribution is broad. As hydrogen is added, the weakest bonds are occupied, making the band tails sharper. At some hydrogen and weak-bond concentration a steady state is achieved, where for each doubly occupied weak bond there is an equivalent lattice distortion creating new weak bonds. The valence-band tail slope is not therefore a function of the defect equilibration process, rather it is a function of the underlying Si lattice and this can depend on deposition conditions in a complex way.

### C. Law of mass action

In order to derive both the electron and hydrogen densities of states, we need to apply the law of mass action to the different chemical equilibria, using the reaction energies. Table I lists the four basic chemical equilibrium equations (3)–(6), together with the reaction energies, expressed both as hydrogen binding energies (as used in the hydrogen density of states) and expressed as electron energies (as used in an electron density of states).  $H_M$  is the energy of a mobile hydrogen atom, while  $H_{\text{SiH}}$  represents the energy of a hydrogen atom in an isolated SiH bond.  $H^{0/1}$  is the energy of the 0/1 transition of a hydrogen atom in a SiSi bond, i.e., when the bond occupancy changes from zero hydrogen atoms to one hydrogen atom or vice versa. Similarly  $H^{1/2}$  is the transition energy when the occupancy changes from 1 to 2 or from 2 to 1.  $H_{\text{av}}$  is the average binding energy of a pair of H atoms in a SiSi bond. It is equal to the average of  $H^{0/1}$  and  $H^{1/2}$ . For the electron energies,  $E$  is the  $+/0$  transition energy of an amphoteric dangling bond, i.e., the change in occupation from zero to one electron or vice versa.  $E_i$  is the energy

of an electron in a SiSi bond,  $E_v$  is the energy of the valence-band mobility edge,  $E_{\text{SiH}}$  is the energy of an electron in a SiH bond, and  $E_{\text{H}_i}$  is the energy of the electron in a mobile, neutral hydrogen atom. As we shall see later, the unknown energies  $E_{\text{H}_i}$  and  $E_{\text{SiH}}$  (used here for simplicity of presentation) can be canceled out by use of the hydrogen chemical potential, which is experimentally measurable.

The reaction energies in Table I all assume that the dangling bond is formed in the neutral state and so contains a single electron. This is modified later, when we introduce the defect-pool model, which allows defects to be formed in all three charge states, and produces very significant effects in the density of states. Additional complications could be introduced by also considering occupation of the tail states, but as we are solving for *equilibrium* distributions (i.e., not under light soaking or carrier stress), it may be shown that this effect is never significant in any physical situation.

The extra strain term in the SiHHSi state is represented by the  $E_v - E_i$  term in the electron energy in reaction (5). The strain term is referenced to the valence-band mobility edge, as unstrained bonds correspond to the extended (mobile) states. A similar term is present in reaction (6), but it is canceled by the  $E_i$  term from Eq. (4), as Eqs. (4)+(5)=(6). This is in agreement with experiment, which shows that reaction (6) contains no net  $E_i$  term; i.e., typical bonds rather than weak bonds are occupied. Thus, both Eqs. (4) and (5) must have an  $E_i$  term.

We first apply the law of mass action to Eq. (6) as follows:

$$\frac{[\text{SiSi}]}{[\text{SiHHSi}]} \frac{[\text{H}_i]^2}{[N_{\text{H}_M}]^2} = \exp\left(\frac{2H_{\text{av}} - 2H_M}{kT}\right). \quad (7)$$

$N_{\text{H}_M}$  is the effective density of hydrogen states at the energy of the hydrogen mobility edge,  $H_M$ . This term is required as a normalization term for the concentration of mobile hydrogen interstitials  $\text{H}_i$ .  $H_{\text{av}}$  is the average binding energy, per hydrogen atom, and since hydrogen binds in pairs to (typical) SiSi bonds, then  $H_{\text{av}}$  is a constant.

We can now define the hydrogen chemical potential ( $\mu_{\text{H}}$ ) by

$$\frac{[\text{H}_i]}{[N_{\text{H}_M}]} = \exp\left(\frac{\mu_{\text{H}} - H_M}{kT}\right). \quad (8)$$

Such a definition is completely analogous to the definition of an electron chemical potential, i.e., the Fermi level, by

$$\frac{[n]}{[N_C]} = \exp\left(\frac{E_F - E_C}{kT}\right), \quad (9)$$

where  $N_C$  is the effective density of conduction-band states at the electron mobility edge  $E_C$ .

If we now substitute Eq. (8) into Eq. (7), we obtain

$$\frac{[\text{SiSi}]}{[\text{SiHHSi}]} = \exp\left(\frac{2H_{\text{av}} - 2\mu_{\text{H}}}{kT}\right). \quad (10)$$

This can be regarded as an alternative form of the law of mass action, where the hydrogen is included implicitly via the hydrogen chemical potential. This is analogous to choosing to use the Fermi level when considering electronic tran-

sitions of defects. In this case, energies are usually considered relative to the Fermi level, rather than considering the concentration of electrons at the mobility edge. The use of a chemical potential is more general, as the precise details of where the hydrogen or electrons are located is irrelevant at equilibrium.

Next, we define  $H$  as the total concentration of hydrogen in the  $a$ -Si:H that exists in pairs in SiSi bonds. We define  $N_{\text{SiSi}}$  as the total number of electrons in the silicon bonding states.  $H$  is about  $5 \times 10^{21} \text{ cm}^{-3}$ , i.e., 10 at. %, as most hydrogen in device quality  $a$ -Si:H is bound in this way.  $N_{\text{SiSi}}$  is  $\sim 2 \times 10^{23} \text{ cm}^{-3}$ , i.e., four electrons per Si atom. Therefore Eq. (10) can be rearranged to give

$$\mu_{\text{H}} = H_{\text{av}} + \frac{kT}{2} \ln\left(\frac{H}{N_{\text{SiSi}}}\right). \quad (11)$$

Substituting the appropriate values for  $H$  and  $N_{\text{SiSi}}$  we find that  $\mu_{\text{H}}$  is strongly pinned about 80 meV below  $H_{\text{av}}$  (taking  $kT$  at freeze-in to be 43 meV, i.e.,  $T=500$  K). A doubling of the hydrogen concentration (to 20 at. %) would result in only about a 15-meV shift in hydrogen chemical potential. A wide range of hydrogen diffusion experiments measure the activation energy of hydrogen diffusion to be  $\sim 1.5$  eV, which corresponds to  $H_M - \mu_{\text{H}}$ .<sup>22,23</sup>

We now apply the law of mass action to Eqs. (3)–(5), this time writing the reaction energy both as hydrogen and electron energy terms:

$$\begin{aligned} \frac{[\text{SiH}]}{[D]} &= \frac{[H_i]}{[N_{H_M}]} \exp\left(\frac{H_M - H_{\text{SiH}}}{kT}\right) \\ &= \frac{[H_i]}{[N_{H_M}]} \exp\left(\frac{E + E_{H_i} - 2E_{\text{SiH}}}{kT}\right), \end{aligned} \quad (12)$$

$$\begin{aligned} \frac{[\text{SiHD}]}{[\text{SiSi}]} &= \frac{[H_i]}{[N_{H_M}]} \exp\left(\frac{H_M - H^{0/1}}{kT}\right) \\ &= \frac{[H_i]}{[N_{H_M}]} \exp\left(\frac{2E_t + E_{H_i} - E - 2E_{\text{SiH}}}{kT}\right), \end{aligned} \quad (13)$$

$$\begin{aligned} \frac{[\text{SiHHSi}]}{[\text{SiHD}]} &= \frac{[H_i]}{[N_{H_M}]} \exp\left(\frac{H_M - H^{1/2}}{kT}\right) \\ &= \frac{[H_i]}{[N_{H_M}]} \exp\left(\frac{E_{H_i} + E - 2E_{\text{SiH}} + 2(E_v - E_t)}{kT}\right). \end{aligned} \quad (14)$$

Equating the hydrogen and electron energy terms from Table I, we can write

$$H_M - H_{\text{SiH}} = E + E_{H_i} - 2E_{\text{SiH}}, \quad (15)$$

$$H_M - H^{0/1} = 2E_t + E_{H_i} - E - 2E_{\text{SiH}}, \quad (16)$$

$$H_M - H^{1/2} = E_{H_i} + E - 2E_{\text{SiH}} + 2(E_v - E_t), \quad (17)$$

$$H_M - H_{\text{av}} = E_{H_i} + E_v - 2E_{\text{SiH}}. \quad (18)$$

When Eqs. (11) and (18) are combined with (15)–(17) we can determine the relations relevant to occupancy of the hydrogen density of states:

$$H_{\text{SiH}} - \mu_{\text{H}} = E_v - E + \frac{kT}{2} \ln\left(\frac{N_{\text{SiSi}}}{H}\right), \quad (19)$$

$$H^{0/1} - \mu_{\text{H}} = E + E_v - 2E_t + \frac{kT}{2} \ln\left(\frac{N_{\text{SiSi}}}{H}\right), \quad (20)$$

$$H^{1/2} - \mu_{\text{H}} = 2E_t - E - E_v + \frac{kT}{2} \ln\left(\frac{N_{\text{SiSi}}}{H}\right). \quad (21)$$

It is of interest to combine (16) and (17) to derive the expression:

$$H^{1/2} - H^{0/1} = 4E_t - 2E - 2E_v. \quad (22)$$

$H^{1/2} - H^{0/1}$  is the difference in transition energies of a SiSi bond undergoing a change of occupancy from one to two hydrogen atoms and a SiSi bond undergoing a change in occupancy from zero to one hydrogen atom. This has been called the hydrogen correlation energy  $U_{\text{H}}$ .<sup>13,16</sup> For most SiSi bonds the hydrogen correlation energy is large and negative, but for bonds in the valence-band tail, it becomes increasingly more positive, until those sites where defects are formed, i.e., a SiSi occupied by one H atom, where the correlation energy is positive.

#### D. Defect pool and the electronic density of states

The key feature of the defect-pool model is that we allow defects to be formed at a range of energies  $E$ , and in all three charge states (+, 0, -). The mean energy of the electrons in the defect depends on the probability of the defect being in each charge state. If the defect is positively charged then the electron has been removed to the Fermi level. If the defect is neutral, then the defect's electron is at the defect energy  $E$ . If the defect is negative, then a second electron is placed on the defect, from the Fermi level, giving a total energy of  $2E - E_F + U$ , where  $U$  is the defect electron correlation energy. We can then calculate the mean defect energy and the mean electron entropy to give the defect chemical potential  $\mu_d$ , which is defined as the free energy per defect.<sup>7,8</sup>

To account for charged defects in the law of mass action equations, then it is necessary to replace  $E$ , the defect energy, with the defect chemical potential,  $\mu_d = E + kT \ln[f^0(E)/2]$ , where  $f^0(E)$  is the neutral occupation function for amphoteric silicon dangling bonds:

$$\begin{aligned} f^0(E) &= \frac{2 \exp([E_F - E]/kT)}{1 + 2 \exp([E_F - E]/kT) + \exp([2E_F - 2E - U]/kT)}. \end{aligned} \quad (23)$$

Note that in our previous work,<sup>7,8</sup>  $\mu_d$  contained an extra term for the hydrogen entropy. Here we deal with the hydrogen entropy implicitly by the use of the law of mass action to the elemental reactions (3)–(5), so the defect chemical potential is defined *without* the explicit hydrogen entropy term.

To allow for distributions of defect energies, i.e., a defect pool, and for distributions of bond energies it is necessary to

replace the single expressions SiHD and SiSi with distribution functions. Therefore we replace [SiSi] by  $g_t(E_t)P(E) - D(E, E_t)$ , where  $g_t(E_t)$  is the one-electron density of states for the valence band,  $P(E)$  is the unit area distribution function for potential defect sites (the defect-pool function), and  $D(E, E_t)$  is the density of defects on (SiHD) sites with energy  $E$  due to bonds of energy  $E_t$ . The expression  $g_t(E_t)P(E)$  is the density of SiSi bonds at energy  $E_t$  that would form a defect at an energy  $E$ . Subtracting  $D(E, E_t)$  allows for the depletion of these SiSi weak bond sites by the defects that have formed.  $g_t(E_t)$  only needs defining in the region of the valence-band tail, as almost all defects occur in this region. We take  $g_t(E_t) = N_{v0} \exp[(E_v - E_t)/E_{v0}]$ , where  $E_{v0}$  is the characteristic energy and  $N_{v0}$  is the density of states of the valence-band tail exponential region extrapolated to the valence-band mobility edge  $E_v$ .  $P(E)$  is usually taken as a Gaussian,  $P(E) = (2\sigma^2\pi)^{-1/2} \exp[-(E - E_p)^2/(2\sigma^2)]$ , where  $\sigma$  is the pool width, and  $E_p$  is the most probable potential defect energy. Remember that  $E$  is the energy of the  $+/0$  transition of the defect. The  $0/-$  transition occurs at an energy  $E + U$ .

We now write down the differential form of the law of mass action in Eq. (13), substituting the expression for the hydrogen chemical potential:

$$D(E, E_t) = [g_t(E_t)P(E) - D(E, E_t)] \exp\left(\frac{\mu_H - H^{0/1}}{kT}\right). \quad (24)$$

This can be rearranged to give

$$D(E, E_t) = \frac{g_t(E_t)P(E)}{1 + \exp[(H^{0/1} - \mu_H)/kT]}. \quad (25)$$

From this point we can either substitute for  $H^{0/1} - \mu_H$  in terms of electron energies, and integrate over the tail states to derive the electronic density of defect states, or we can substitute for the electronic energies and integrate to get the hydrogen density of states multiplied by an occupation function.

First we derive the electronic density of defect states by substituting using Eq. (20) and integrating over the bond energy distribution, using a similar method as previously:<sup>7,8</sup>

$$D(E) = \int \frac{g_t(E_t)P(E)}{1 + \exp\{[E + E_v - 2E_t + (kT/2)\ln(N_{\text{SiSi}}/H)]/kT\}} \times dE_t. \quad (26)$$

Substituting for the exponential tail state distribution and performing the integral leads to the following result for the density of defect states:

$$D(E) = \gamma \left(\frac{2}{f^0(E)}\right)^{kT/2E_{v0}} P\left(E + \frac{\sigma^2}{2E_{v0}}\right), \quad (27)$$

$$\gamma = N_{v0} \left(\frac{H}{N_{\text{SiSi}}}\right)^{kT/4E_{v0}} \left(\frac{2E_{v0}^2}{2E_{v0} - kT}\right) \times \exp\left[-\frac{1}{2E_{v0}} \left(E_p - E_v - \frac{\sigma^2}{4E_{v0}}\right)\right]. \quad (28)$$

This result is similar to our earlier expression for  $D(E)$ ,<sup>7,8</sup> but  $E_{v0} + ikT/2$  has been replaced by  $2E_{v0}$ , and there are changes to the energy-independent prefactor  $\gamma$  that reduce the overall density of states by a factor of about 3.

Expressions (27) and (28) give the density of defect states, corresponding to SiSi bonds occupied by a single hydrogen atom, i.e., SiHD states. This does not include defects on isolated SiH bonds, i.e.,  $D$  defects, which could be calculated separately, using Eq. (12). Since the density of isolated SiH sites is about  $10^{20} \text{ cm}^{-3}$ , and since the binding energy of the hydrogen in a SiH bond is higher than H in a weak SiSi bond, we find that the density of the  $D$  defects is several orders of magnitude lower than the density of the SiHD defects, and so the total defect density is always dominated by the SiHD states.

### E. Hydrogen density of states

If we now return to Eq. (25), we can substitute for the electron energies and derive the hydrogen density of states, which is completely consistent with the electronic density of states incorporating the defect-pool model. By substituting for  $E_t$  in terms of  $E$  and  $H^{0/1}$ , and then integrating over  $E$ , Eq. (25) becomes the hydrogen density of states multiplied by a Fermi occupation function:

$$D(H^{0/1}) = \frac{h^{0/1}(H^{0/1})}{1 + \exp\left[\frac{(H^{0/1} - \mu_H)}{kT}\right]}, \quad (29)$$

where  $h^{0/1}(H^{0/1})$  is the hydrogen density of states, i.e., the total density of hydrogen 0/1 transitions at a hydrogen binding energy  $H^{0/1}$ ;

$$h^{0/1}(H^{0/1}) = \int g_t \left( \frac{H_{\text{av}} - H^{0/1} + E + E_v + kT \ln[f^0(E)/2]}{2} \right) \times P(E) dE. \quad (30)$$

In the same way as we derived Eq. (24) from (13) we can derive from (14):

$$D(E, E_t) = \frac{H}{N_{\text{SiSi}}} [g_t(E_t)P(E) - D(E, E_t)] \exp\left(\frac{H^{1/2} - \mu_H}{kT}\right). \quad (31)$$

Here the  $H/N_{\text{SiSi}}$  term comes from the fact that only this fraction of bond states are doubly hydrogenated. If this term is taken inside the exponent, then we obtain a similar expression to (29), for the density of defects:

$$D(H^{1/2}) = \frac{h^{1/2}(H^{1/2})}{1 + \exp\{[H^{1/2} - \mu_H - kT \ln(H/N_{\text{SiSi}})]/kT\}}, \quad (32)$$

where we define the density of states for the  $H^{1/2}$  transition by

$$h^{1/2}(H^{1/2}) = \int g_t \left( \frac{H^{1/2} - H_{\text{av}} + E + E_v + kT \ln[f^0(E)/2]}{2} \right) \times P(E) dE. \quad (33)$$

Note that due to the  $H/N_{\text{SiSi}}$  term in Eq. (31) the  $h^{1/2}$  transition has an effective chemical potential of  $\mu_H + kT \ln(H/N_{\text{SiSi}})$ . This is a degeneracy term due to the fact that for each bond that is doubly hydrogenated, there are many more that are identical but empty. Strictly speaking, a similar term should exist in the  $h^{0/1}$  transition level, but as almost all bonds are empty, this is insignificant. This is like the degeneracy term for electron occupation statistics of a dangling bond, where the spin degeneracy term results in a chemical potential given by  $E_f + kT \ln(2)$  for the  $D^{+/0}$  transition, and  $(E_f - U) - kT \ln(2)$  for the  $D^{0/-}$  transition.<sup>7,8</sup>

### III. CALCULATED ELECTRONIC DENSITY OF STATES

Using the new expression for the density of electronic states, given in Eqs. (27) and (28), we can now evaluate the expression for both intrinsic and doped amorphous silicon. The method is substantially the same as described in our previous paper,<sup>8</sup> except that the revised expression leads to about a factor of 3 lower densities and we have chosen to revise some of the input parameters so as to give better fits to experimental results. Most parameters are identical to those used previously,<sup>8</sup> in particular, we take  $N_{v0} = 2 \times 10^{21} \text{ cm}^{-3} \text{ eV}^{-1}$ ,  $H = 5 \times 10^{21} \text{ cm}^{-3}$ ,  $E_G$  (the band gap) = 1.9 eV,  $T^* = 500 \text{ K}$ , and the correlation energy  $U = 0.2 \text{ eV}$ . However, we now take  $\sigma$  to be 0.190 eV, compared to 0.178 eV used previously. The value of  $\sigma$  is chosen to keep the energy separation between the  $D_e^-$  and  $D_h^+$  states to be 0.44 eV, in agreement with experiment, as before,<sup>8</sup> but due to the new expression for  $D(E)$ , this now leads to the new value. We take the room-temperature value for  $E_{v0}$  to be 0.045 eV, which is typical for good quality material and we allow for the temperature dependence in  $E_{v0}$ , by  $E_{v0}^2 = E_{v0}^2_{T=0} + (kT)^2$ ,<sup>24</sup> so  $E_{v0}$ , at the  $T^* = 500 \text{ K}$  equilibrium temperature, is 0.056 eV.

Compared to the numerical results presented in our previous paper,<sup>8</sup> the main changes are the factor of 3 lower defect densities, a small change in the energy spectra, due to the increased  $\sigma$ , and a lower thermal activation energy of the neutral spin density ( $D^0$  states). We now find a thermal activation energy of the  $D^0$  states of 0.27 eV, compared to the earlier reported 0.39 eV. This gives somewhat better agreement with experiment, which finds a range of activation energies from 0.18 eV,<sup>3</sup> through 0.3 eV,<sup>25</sup> to 0.35 eV.<sup>26</sup>

Calculations using the above parameters represent state of the art high-quality amorphous silicon, with state of the art low defect densities. This does not cover all intrinsic material and we handle poorer quality material by simply increasing  $E_{v0}$ , the valence-band tail slope. However, we also increase  $\sigma$  in such a way that the energy position of the  $D^-$  and  $D^+$  peaks is kept constant,<sup>8</sup> which is consistent with experiment. Both  $E_{v0}$  and  $\sigma$  are disorder parameters and it seems reasonable that they should change together.

Figure 1 shows the dependence of the total defect density on the room-temperature valence-band tail slope,  $E_{v0}$ , and the comparison with experimental data, taken from a data compilation in Stutzmann.<sup>27</sup> Exactly how  $E_{v0}$  is varied is outside the scope of our model, since  $E_{v0}$  is merely an input parameter. However, experimentally, we find increased  $E_{v0}$  for deposition at reduced temperatures, or at higher tempera-

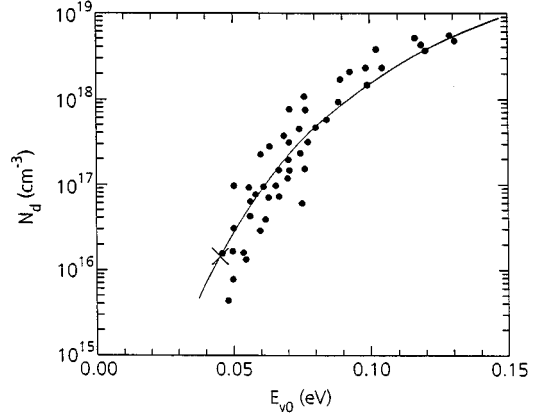


FIG. 1. The dependence of the total defect density  $N_d$  on the valence-band tail slope,  $E_{v0}$ , compared to experimental data compiled by Stutzmann (Ref. 27). Data point marked with a cross results from the model parameters used in this paper.

tures with low hydrogen content and generally at less than optimum deposition conditions.<sup>27</sup>

There is good agreement between experiment and theory, both in the magnitude of the defect densities and in the  $E_{v0}$  dependence. Remember these are room-temperature measurements of  $E_{v0}$ , not  $E_{v0}^*$ , which is the value at the equilibrium temperature, and that the spin density is about a factor of 5 lower than the defect density. Included in Fig. 1 is the single point, representing our model. Clearly this set of parameters represents state of the art amorphous silicon.

When the amorphous silicon is doped, then the density of  $D_e$  states (for  $n$  type) or  $D_h$  states (for  $p$  type) increases exponentially with the shift in Fermi level and dominates the total defect density.<sup>8</sup> With the new expression for  $D(E)$ , the Fermi-level dependence of the total defect density is given (for  $n$  type) by

$$D_e \approx \exp(E_F/2E_{v0}^*), \quad (34)$$

with a similar expression for  $D_h$  states in  $p$ -type material. The characteristic temperature  $2E_{v0}^*$  (112 meV) agrees well with experiment, where 100 meV is found.<sup>28</sup>

We now discuss two interesting consequences of the defect-pool model, not discussed in our previous paper.<sup>8</sup> These are the statistical shift and the defect density profile in junction devices. Figure 2 shows the density of states for lightly doped  $n$ -type  $a$ -Si:H, with the equilibrium Fermi level,  $E_F^* = 1.30 \text{ eV}$ . For highly doped  $n$ -type  $a$ -Si:H, the density of  $D_e$  states increases and the Fermi level rises into the conduction-band tail states. Therefore, the Fermi level can be in a region where the density of states is either increasing or decreasing with energy and this leads to different behaviors for the temperature dependence of the Fermi level, known as the statistical shift. In Fig. 3, we plot the statistical shift for lightly doped  $a$ -Si:H (as in Fig. 2) as well as for more heavily doped  $a$ -Si:H. For the lightly doped  $n$ -type  $a$ -Si:H, the statistical shift of the Fermi level is positive at low temperatures and changes sign at higher temperatures, whereas for the highly doped  $a$ -Si:H, the statistical shift is negative. Proper account of the statistical shift is needed to

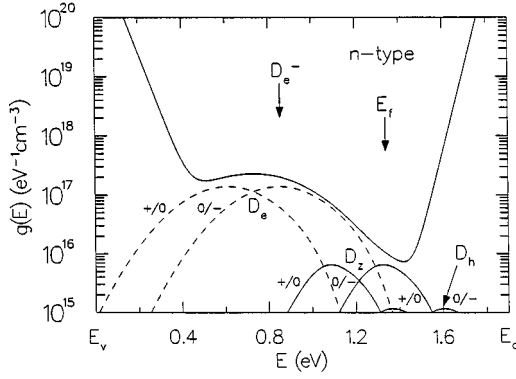


FIG. 2. The one-electron density of states for lightly doped  $n$ -type  $a$ -Si:H. The equilibrium Fermi level is shifted by 0.25 eV from the intrinsic position but the Fermi energy is shown at 313 K.

relate room-temperature Fermi levels to equilibrium temperature Fermi levels and to conductivity activation energies.

Figure 4 shows the dependence of the  $n$ -type active-dopant level,  $N_{\text{donor}}$  (identically equal to the net negatively charged dangling-bond defect density,  $D_e - D_h$ ) on the conductivity activation energy. There is an extremely nonlinear response that is due to the statistical shift increasing at the point where the activation energy changes strongly with little change in the active-dopant level. This curve shows that a 1 part per  $10^6$  active-doping level ( $N_{\text{donor}} = 5 \times 10^{16} \text{ cm}^{-3}$ ) would correspond to a Fermi-level shift of about 0.2 eV, in reasonable agreement with experiment.<sup>29,30</sup> At the higher doping levels, we find an activation energy of about 0.15 eV, for  $2 \times 10^{18} \text{ cm}^{-3}$  active dopants. In the model,  $E_{v0}$  is assumed constant, but there is some experimental evidence that  $E_{v0}$  actually increases with doping, at the higher doping levels.<sup>28</sup> We presume this effect is due to increased disorder in the presence of a large concentration of dopant atoms, remembering that the number of dopant atoms is roughly the square of the number of active dopants, for high doping levels.<sup>31</sup> In Fig. 4, we also plot by the dotted line,  $E_F^*$ , as a function of conduction activation energy, which illustrates the effect of the statistical shift more directly.

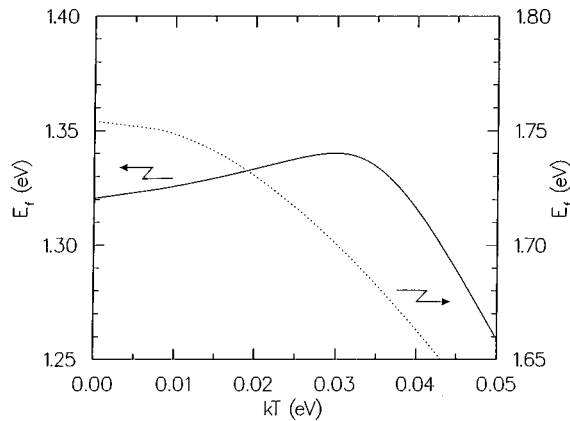


FIG. 3. The calculated statistical shift of the Fermi energy, for lightly doped  $a$ -Si:H (as shown in Fig. 2) (solid line) and more highly doped  $a$ -Si:H (dotted line).

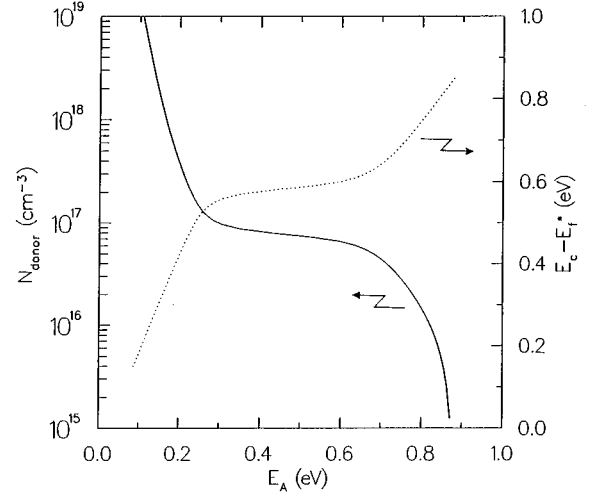


FIG. 4. The active-dopant level dependence on the activation energy of conduction for  $n$ -type conduction. Also shown by the dotted line is the equilibrium Fermi-level position, as a function of the activation energy of conduction.

Figure 5 shows the band-bending potential profile and the equilibrium defect density, through the  $i$ -layer region of a pin diode. We adopt the usual convention that  $\psi$  is positive for positive band bending, which is drawn increasing downwards. Thus we plot the energy band-bending profile through a pin diode, with the  $p$ - $i$  interface at the left side and the  $n$ - $i$  interface at the right side. The density of states will equilibrate to the Fermi-level position at the equilibration temperature throughout the  $1.0 \mu\text{m}$ -thick  $i$  layer, and so the defect density will vary through the thickness of the  $i$  layer, as shown in the figure. We find the density of defects stays approximately constant throughout most of the thickness of the  $i$  layer, but increases rapidly towards the  $n$ - $i$  and  $p$ - $i$  interfaces, where it increases over an order of magnitude. This inhomogeneity in the defect density leads to an increase in the field near to the  $n$ - $i$  and  $p$ - $i$  interfaces and a corre-

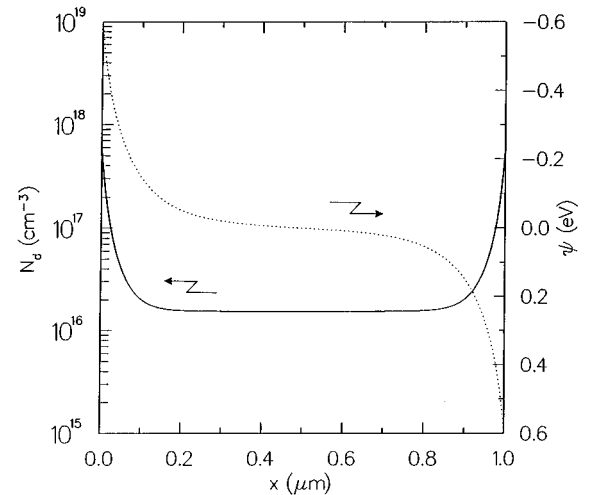


FIG. 5. Equilibrium defect density profile (solid line) and band-bending potential profile (dotted line) through the  $i$ -layer region of an equilibrated  $pin$  diode, according to our defect-pool model.

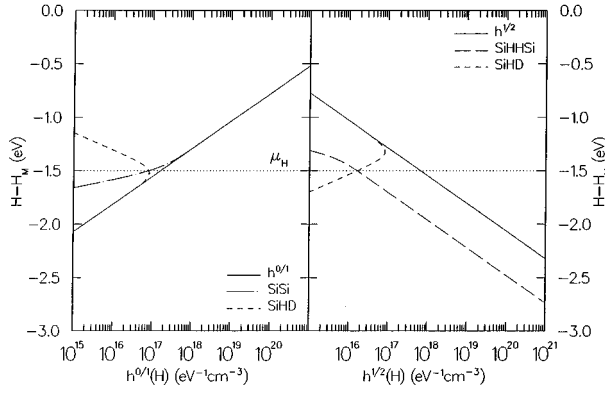


FIG. 6. The hydrogen density of states for intrinsic  $a$ -Si:H. The left part depicts  $h^{0/1}$  transitions and the right depicts  $h^{1/2}$  transitions. The solid line represents all potential transitions, while the other lines show allowed transitions. Thus only SiSi and SiHD may undergo  $0/1$  transitions, while only SiHD and SiHHSi may undergo  $1/2$  transitions.

sponding decrease in the field in the center of the  $i$  layer, compared to the non-defect-pool model situation with a homogeneous defect distribution. The band-bending potential profile is shown at  $T=313$  K, which differs from the equilibrium band-bending profile at  $T=500$  K, due to the statistical shift. This latter effect causes the field in the center of the diode to be larger at room temperature, than it is at the equilibration temperature and we can see that there is a noticeable field at the center of the diode. This field leads to the high zero-bias quantum efficiency, which is measured in solar cells.

#### IV. CALCULATED HYDROGEN DENSITY OF STATES

##### A. Hydrogen density of states curves

Figure 6 shows the calculated hydrogen density of states. The  $h^{0/1}$  and  $h^{1/2}$  distributions are shown separately, but the distributions of defect states SiHD appear in both distributions. Also shown are the distributions of SiSi and SiHHSi states. The defect states in the  $h^{0/1}$  distribution exist in the part of the band tail that extends below  $\mu_H$ , together with an exponential tail above  $\mu_H$ . Similarly, the same defect states appear in the  $h^{1/2}$  distribution, above  $\mu_H + kT \ln(H/N_{\text{SiSi}})$  and in an exponential tail to lower energies. Note that  $h^{0/1}$  and  $h^{1/2}$  include all possible sites. This is nearly the same as SiSi for the  $h^{0/1}$  distribution above  $\mu_H$ , but SiSi is depleted by the formed defects below  $\mu_H$ . On the other hand, SiHHSi is a constant fraction of the  $h^{1/2}$  distribution below  $\mu_H$  and this is further depleted by the SiHD states above  $\mu_H + kT \ln(H/N_{\text{SiSi}})$ .

It is important to realize that the SiHD states are the *same* states in the  $h^{0/1}$  and  $h^{1/2}$  distributions. The SiHD states are amphoteric to H occupancy, in a similar way that the  $D(E)$  states are amphoteric to electron occupancy. The total density of SiHD states, i.e., the integral of SiHD in the hydrogen density of states is identical to the integral of  $D(E)$  in the electron density of states.

To understand the origin of the hydrogen density of states (HDOS) it is instructive to calculate it for two simplified situations. Firstly, we can calculate it for the case where there

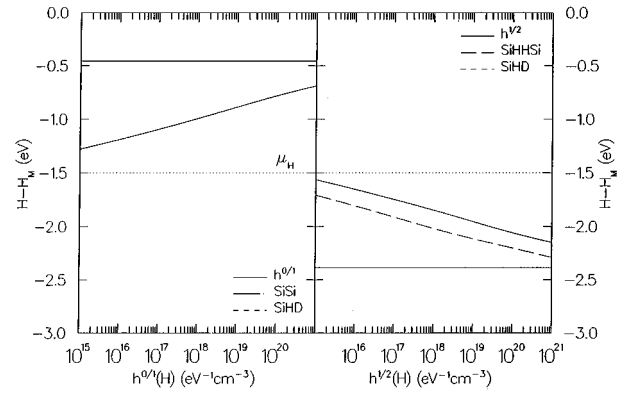


FIG. 7. The hydrogen density of states, for intrinsic  $a$ -Si:H in a model where there are no SiSi tail states.

are no tail states, i.e.,  $E_t=0$ , so all electrons in SiSi bonds have the same energy. The second situation is where there is no defect pool, i.e., where  $P(E)$  is a  $\delta$  function and all the defects occur at a single electronic energy,  $E'$ . It is also interesting to show how the total density of states divides into states of different potential charge state. We can define the hydrogen density of states that would form defects in the negative charge state by

$$h_e^{0/1} = \int g_t \left( \frac{H_{\text{av}} - H^{0/1} + E + E_v + kT \ln[f^0(E)/2]}{2} \right) \times P(E) f^-(E) dE, \quad (35)$$

with similar expressions for neutral ( $h_z^{0/1}$ ) and positive ( $h_h^{0/1}$ ) charge states.

Figure 7 shows the hydrogen density of states, when there are no SiSi electron tails. Compared to Fig. 6, the hydrogen density of states shows a small amount of structure, which can be identified with the different charge states having different hydrogen binding energy dependence. Also shown is the energy cutoff of the hydrogen density of states, which occurs in a model with no tail states. As we might expect, the overall density of states shows reduced tailing and the density of defect states (SiHD) is too low to be shown.

Figure 8 shows the hydrogen density of states when there are tails but no defect pool. Comparison with Fig. 6 shows

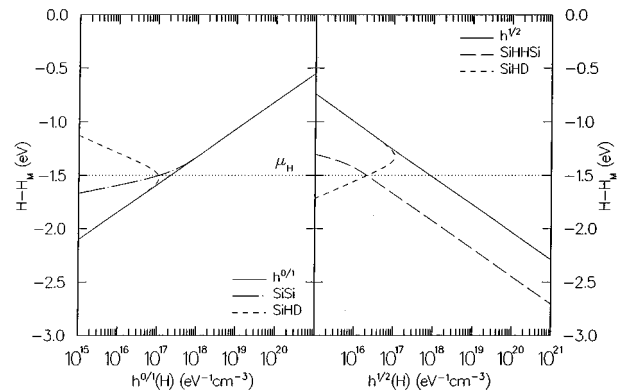


FIG. 8. The hydrogen density of states, for intrinsic  $a$ -Si:H, in a model where there are tail states, but no defect pool.



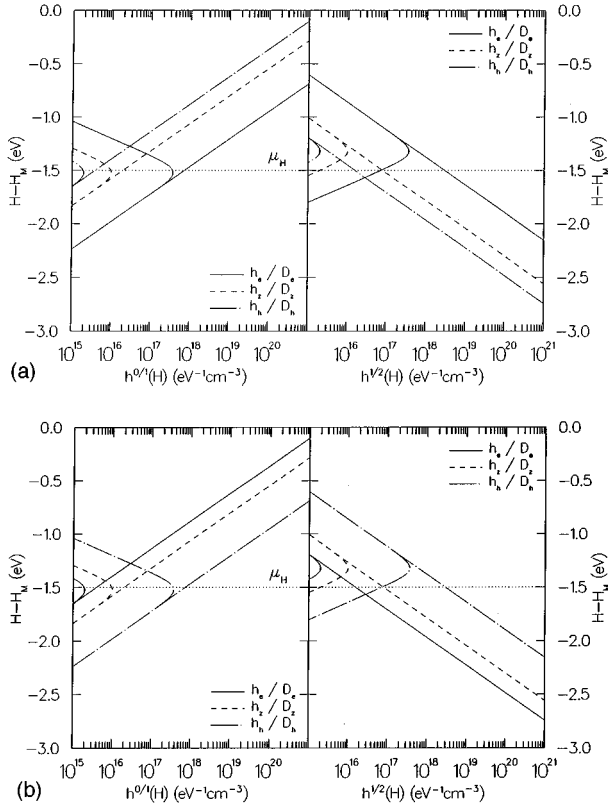


FIG. 9. The hydrogen density of states in the full model, for (a) *n*-type and (b) *p*-type *a*-Si:H, showing the division into potential states of different charge state.

that the density of states has the same general shape as in the full model. The only real difference is that with no pool, the vast majority of states are neutral, whereas in the full model, the majority of states occur either as positive or negative. We therefore conclude that the hydrogen density of states is dominated by the tail state distribution and the only effect of the defect pool is to determine the charge state of the defects and potential defect sites. This can be contrasted with the effect of the defect pool on the electronic density of states, where the density of states is completely modified by the effect of the defect pool.

Figure 9 shows the full model hydrogen density of states for (a) *n*-type and (b) *p*-type *a*-Si:H. The density of states and the corresponding density of defects is increased by doping. The vast majority of defect states and potential defect states are negatively charged, for *n*-type material, but the opposite is true for *p*-type material. The hydrogen densities of states in Fig. 9(a) correspond to the electron density of states shown in Fig. 2 and the integrated defect densities are identical.

By way of comparison, Fig. 10 shows the calculated density of states for (a) *n*-type and (b) *p*-type material, for the no-tail model. Compared to Fig. 9, there is a strong asymmetry in the densities, between *n*-type and *p*-type material, due to the broader distribution of  $h_e$  states compared to the  $h_h$  states. Note that the energy position of the cutoff is Fermi energy dependent. In the full model, the effect of the tail is dominant and the asymmetry between *n*-type and *p*-type distribution is lost.

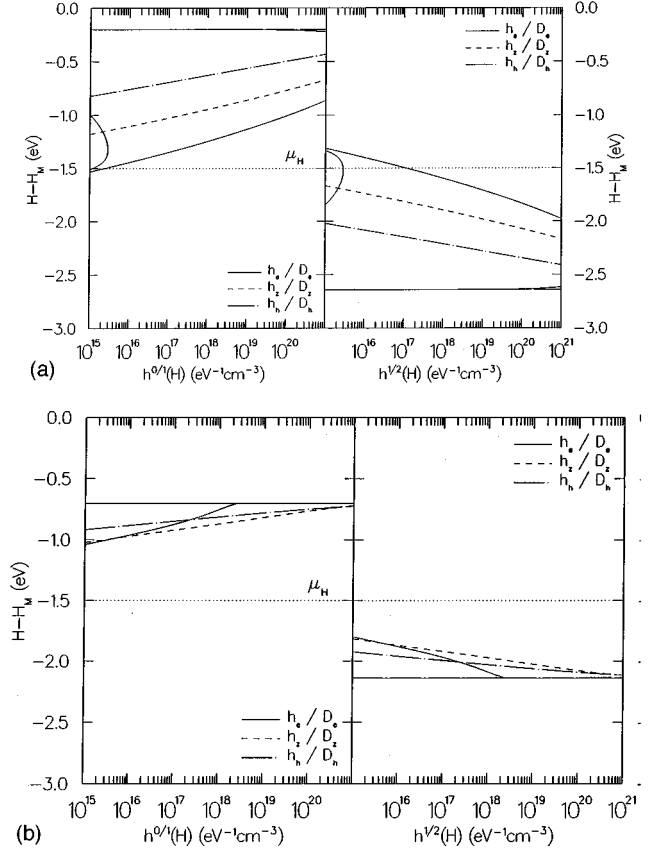


FIG. 10. The hydrogen density of states, for (a) *n*-type and (b) *p*-type *a*-Si:H, in a model where there are no tail states, showing the division into potential states of different charge state.

## B. Comparison with experiment

As we have derived it, the HDOS shows how *a*-Si:H is relatively insensitive to the addition or subtraction of quite large amounts of hydrogen, for example, in hydrogenation and dehydrogenation experiments.<sup>20,21</sup> In hydrogenation, the hydrogen chemical potential is virtually pinned and there is no change in the defect density. In dehydrogenation, the hydrogen chemical potential will also be pinned until almost all the hydrogen is removed, i.e., except for the hydrogen located on isolated SiH bonds. The hydrogen chemical potential drops towards the SiH level, whereupon the defect density from empty SiSi bonds reduces slightly and hydrogen is slowly emitted from the isolated SiH sites. At this point, the defect density rises sharply, due to one of two reasons; either there is an increase in the spin density from isolated SiH sites that have lost a hydrogen atom, or there is an increase in  $E_{v,0}$ , due to an increase in disorder, as the last hydrogen is evolved, and the density of spins from singly occupied SiSi states increases. This is consistent with experimental measurements of the spin density on dehydrogenation.<sup>32</sup>

Hydrogen diffusion can also be understood with the hydrogen density of states. Hydrogen moves by thermal emission from SiHHSi states to the mobility edge,  $H_M$ . Long-range motion occurs then by a series of capture and emission events within the SiSi band states. The thermal activation energy for hydrogen diffusion is given by  $H_M - \mu_H$ , by analogy with the process of steady-state electrical conduction, which has an activation energy of  $E_c - E_F$ . The position of

$\mu_{\text{H}}$  is taken to give a diffusion activation energy of 1.5 eV, in agreement with the thermal activation energy found in a wide range of diffusion experiments.<sup>23</sup>

Our model presented here has the primary defect site as the SiHD, a singly hydrogenated weak SiSi bond. There is some controversy with this, as several electron spin resonance (ESR) and nuclear magnetic resonance (NMR) experiments have shown no dangling-bond–hydrogen spin interaction. Indeed some claim that there is no significant hydrogen density within 5 Å of a dangling bond, implying an anticorrelation of hydrogen and defects.<sup>33,34</sup> However, we feel there are problems with this concept. Given that device grade *a*-Si:H typically contains  $5 \times 10^{21} \text{ cm}^{-3}$  hydrogen, a 5 Å sphere around each H atom does not leave any room for the dangling bonds. Additionally, if most hydrogen were bound as isolated SiH bonds, then a defect would result for each hydrogen removed, in clear contradiction to experiment,<sup>13,20,21</sup> where several orders of magnitude more hydrogen is removed than there are defects created. A possible explanation is that these experiments are measuring surface spin signals, where the surfaces are likely to have a hydrogen deficit. ESR and NMR experiments are usually performed on powdered samples, formed by depositing on aluminum foil, which is subsequently dissolved. These generally exhibit surface spin signals of  $10^{12} \text{ cm}^{-2}$ ,<sup>35</sup> so for device grade *a*-Si:H, the films would have to be several tens of micrometers thick to actually be measuring *bulk* spins. Such films are difficult to grow due to the internal stresses involved and long times required. An alternative approach is to raise the bulk spin density by lowering the deposition temperatures, and while we should be a little cautious as this material is likely to contain some microvoids, indeed the dangling-bond–hydrogen interaction is seen for a large fraction of the native and light-induced dangling bonds both in NMR (Ref. 36) and ESR,<sup>37</sup> and a dangling–bond–hydrogen,<sup>36,37</sup> separation of about 2 Å is measured, in agreement with our model.

## V. COMPARISON WITH OTHER MODELS

In this section, we compare the details of our model with those of previous work, in order to pinpoint the differences. There are two broad categories of model that we wish to compare: defect-pool models and hydrogen density of states models.

### A. Defect-pool models

In our earlier paper, we discuss the differences between the early papers on the defect-pool model.<sup>8</sup> In this paper, we discuss the specific differences between more recent papers on the defect-pool model and the model presented in this work. The common feature of the previous defect-pool models is that they all consider chemical reactions of the type given in Eqs. (1) and (2) and then attempt to apply the law of mass action to these equations. The problem lies in the fact that Eqs. (1) and (2) strictly only apply if not more than one species on each side of the reaction is *immobile*. As we have previously discussed, this is not really correct. Alternatively, if the chemical reaction describes a purely local reaction where the SiH bonds are neighboring to the SiSi bonds, then

the reactions describe H bond flipping into a neighboring SiSi site. In this case, since reactants and products are intimately linked, the law of mass action does apply, but only if reactants and products are treated as a single species, strongly reducing any entropy terms. This is a perfectly valid, but different, model for defect creation, which would result in far too few defects. The much larger defect densities that are observed experimentally originate from the increase in entropy due to the H motion between neighboring sites. The only correct way to solve this problem is to recognize that H is the truly mobile species and solve Eqs. (3)–(5), as we have done in this paper. The interesting feature of the previous defect-pool models is how they handled the H entropy problem.

Winer<sup>6</sup> considered Eq. (1) and applied the law of mass action. The hydrogen entropy was included, but calculated incorrectly assuming the defect gained entropy from all SiH sites, rather than from only those at the same energy. Schumm<sup>38</sup> considered an essentially local model and allowed energy exchange between the defects, which were formed in pairs. This treatment is basically correct for a local reaction. Hydrogen entropy was then calculated, allowing defect sites to exchange with SiH sites at the same energy. However, all the hydrogen entropy was assigned to only one of the two formed defects, which led to the result that the energy spectrum of the density of states was independent of the choice of specific reaction (1) or (2). In our earlier paper,<sup>8</sup> we recognized that the physical picture we wished to model was of a delocalized formation of pairs of defects. We therefore assigned the two defects the *same* energy, on the basis that the two defects were formed independently and on average they would have the same energy. This enabled us to produce an analytical solution for the density of states, which had some of the features of a delocalized reaction. The calculated energy spectrum of the density of states was found to be different for reactions (1) and (2).<sup>8</sup>

Both the papers of Schumm<sup>38</sup> and our earlier papers<sup>7,8</sup> are flawed when applied to trying to solve reactions (1) and (2) for a delocalized reaction. Neither model handles the hydrogen entropy properly, since the only way to model a delocalized reaction is to decouple it into the correct microscopic components, namely, Eqs. (3)–(5). The distinction between there being one SiH bond or two SiH bonds mediating the defect forming reaction then disappears.

Asensi and Andreu<sup>39</sup> were the first to combine the defect-pool model with elemental hydrogen reactions. However, they did not solve the complete set of equations (3)–(5), instead they solved a simplified version, using Eq. (3) with Eq. (6). They recognized that most hydrogen binds in the network in pairs, but by using Eq. (6) they allowed hydrogen in SiSi bonds to have occupancy of *only* zero or two. Occupancy by a single H atom, in a defect forming site (SiHD) was disallowed. In their model, all defects were formed from reaction (3) on isolated SiH bonds. The resulting energy spectrum of the formed defects gave an energy separation between the  $D_e^-$  and  $D_h^+$  of  $2\sigma^2/kT^* - U$ , independent of the valence-band tail slope  $E_{v0}$ , and an increase of the defect density upon doping with a characteristic energy of  $kT^*$  ( $\sim 43 \text{ meV}$ ), far too steep compared to experiment.<sup>28</sup>

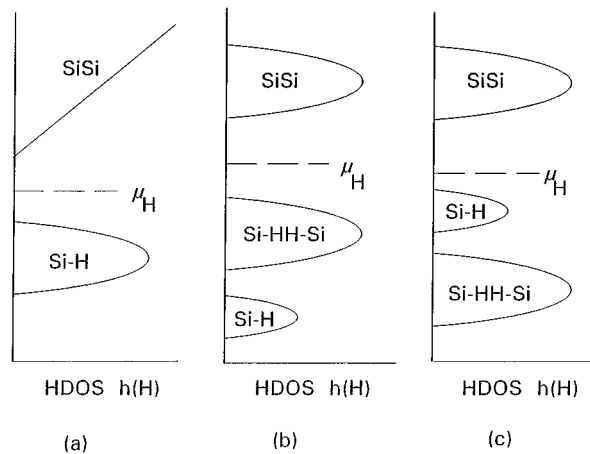


FIG. 11. Hydrogen density of states models: (a) according to Street (Refs. 15 and 16), (b) according to Jackson (Refs. 12 and 19), and (c) according to Zafar and Schiff (Refs. 13 and 32).

### B. Hydrogen density of states models

The concept of the hydrogen density of states was introduced by Street.<sup>15,16</sup> His original model is as sketched in Fig. 11(a). The distinction between SiH and SiHHSi was either not made or they were lumped together. The tail state energy was contained in the SiSi states. Jackson<sup>12,19</sup> introduced the distinction of the SiHHSi states and placed them at a higher energy than the isolated SiH, but neglected the tail state energy [Fig. 11(b)]. The SiHHSi states were identified with the specific  $H_2^*$  configuration.<sup>14,40</sup> Zafar and Schiff<sup>13,32</sup> reversed the order of the SiHHSi and SiH states, so all the defects are formed in isolated SiH states [Fig. 10(c)]. This is the same model used later by Asensi and Andreu.<sup>39</sup>

None of the HDOS models incorporated the defect-pool model, prior to the paper by Asensi and Andreu,<sup>39</sup> but it is of interest to consider the result we would obtain if we were to do this. The Street model basically consists of solving Eqs. (3) and (4). The defects are of two distinct types, located

either on an isolated SiH site or in a SiSi weak-bond site. If this problem is solved properly, the energy spectra of the two defects would be different, with the energy shift between the  $D_e^-$  and the  $D_h^+$  states being  $2\sigma^2/kT^* - U$ , for defects originating from isolated SiH and  $\sigma^2/E_{v0} - U$ , for defects originating from SiSi weak bonds. For a localized reaction, which is represented on the same HDOS by a hydrogen transition directly from the SiH state to the SiSi state, we obtain for the energy separation,  $\sigma^2/E_{v0} - U$ , for both defects, which is the same answer as obtained by Schumm.<sup>38</sup> In the HDOS models of Jackson<sup>12,19</sup> and Zafar and Schiff,<sup>13,32</sup> since no tail states are included, the energy spectra of all defect states will be the same, with a characteristic energy separation of  $2\sigma^2/kT^* - U$ .

In our new model, the energy separation of the  $D_e^-$  and  $D_h^+$  states is  $\sigma^2/E_{v0} - U$ , which is the same answer as obtained in the local model of Schumm.<sup>38</sup> However, the agreement with Schumm<sup>38</sup> is coincidental, since it is actually due to the fortuitous cancellation of two differences, the use of a local model and the incorrect calculation of H entropy. The  $\gamma$  term, which gives the absolute defect densities, according to Eq. (28), is different from the  $\gamma$  terms given in both Schumm<sup>38</sup> and Deane and Powell.<sup>7,8</sup>

## VI. CONCLUSIONS

We have developed a model for the hydrogen density of states that incorporates the defect-pool model for the electronic density of silicon dangling-bond defect states.

The hydrogen density of states has been described in a quantitative way, and shown to reproduce the density of states of the defect-pool model. It is somewhat different from an electronic density of states in that the correlation energy of hydrogen in a silicon-silicon bond varies. It is *positive* for most sites that form defects, but *negative* for most sites that bind hydrogen. In device quality *a*-Si:H, the majority of defects result from singly hydrogenated silicon-silicon bonds, which we term (SiHD), rather than isolated SiH sites.

- <sup>1</sup>R. A. Street, J. Kakalios, C. C. Tsai, and T. M. Hayes, Phys. Rev. B **35**, 1316 (1987).
- <sup>2</sup>R. A. Street, M. Hack, and W. B. Jackson, Phys. Rev. B **37**, 4209 (1988).
- <sup>3</sup>R. A. Street and K. Winer, Phys. Rev. B **40**, 6236 (1989).
- <sup>4</sup>M. Stutzmann, Philos. Mag. B **56**, 63 (1987).
- <sup>5</sup>Y. Bar-Yam and J. D. Joannopoulos, J. Non-Cryst. Solids **97-98**, 467 (1987).
- <sup>6</sup>K. Winer, Phys. Rev. B **41**, 12 150 (1990).
- <sup>7</sup>S. C. Deane and M. J. Powell, Phys. Rev. Lett. **70**, 1654 (1993).
- <sup>8</sup>M. J. Powell and S. C. Deane, Phys. Rev. B **48**, 10 815 (1993).
- <sup>9</sup>J. Kakalios, R. A. Street, and W. B. Jackson, Phys. Rev. Lett. **59**, 1037 (1987).
- <sup>10</sup>W. B. Jackson, J. M. Marshall, and M. D. Moyer, Phys. Rev. B **39**, 1164 (1989).
- <sup>11</sup>R. A. Street, Physica B **170**, 69 (1991).
- <sup>12</sup>W. B. Jackson and C. C. Tsai, Phys. Rev. B **45**, 6564 (1992).
- <sup>13</sup>S. Zafar and E. A. Schiff, Phys. Rev. B **40**, 5235 (1989).
- <sup>14</sup>W. B. Jackson, Phys. Rev. B **41**, 10 257 (1990).
- <sup>15</sup>R. A. Street, Solar Cells **30**, 207 (1991).
- <sup>16</sup>R. A. Street, in *Amorphous Silicon Materials and Solar Cells*, edited by Byron L. Stafford, AIP Conf. Proc. No. 234 (AIP, New York, 1991), p. 21.
- <sup>17</sup>R. A. Street, Phys. Rev. B **44**, 10 610 (1991).
- <sup>18</sup>S. C. Deane and M. J. Powell, in *Amorphous Silicon Technology—1994*, edited by E. A. Schiff *et al.*, MRS Symposia Proceedings No. 336 (Materials Research Society, Pittsburgh, 1994), p. 147.
- <sup>19</sup>W. B. Jackson, *Transport Correlation and Structural Defects* (World Scientific, Singapore, 1990), p. 63.
- <sup>20</sup>N. H. Nickel and W. B. Jackson, J. Non-Cryst. Solids **164-166**, 281 (1993).
- <sup>21</sup>N. H. Nickel and W. B. Jackson, Phys. Rev. B **51**, 4872 (1995).
- <sup>22</sup>R. A. Street, C. C. Tsai, J. Kakalios, and W. B. Jackson, Philos. Mag. B **56**, 305 (1987).
- <sup>23</sup>W. B. Jackson, J. Non-Cryst. Solids **164-166**, 263 (1993).
- <sup>24</sup>M. Stutzmann, Philos. Mag. Lett. **66**, 147 (1992).
- <sup>25</sup>Z. E. Smith and S. Wagner, in *Amorphous Silicon and Related*

- Materials*, edited by H. Fritzsche (World Scientific, Singapore, 1989), p. 409.
- <sup>26</sup>T. J. McMahon, in *Amorphous Silicon Materials and Solar Cells* (Ref. 16), p. 83.
- <sup>27</sup>M. Stutzmann, *Philos. Mag. B* **60**, 531 (1989).
- <sup>28</sup>K. Pierz, W. Fuhs, and H. Mell, *Philos. Mag. B* **63**, 123 (1991).
- <sup>29</sup>M. Hack and R. A. Street, *Appl. Phys. Lett.* **53**, 1083 (1988).
- <sup>30</sup>E. Sauvain, P. Pipoz, A. Shah, and J. Hubin, *J. Appl. Phys.* **75**, 1722 (1994).
- <sup>31</sup>R. A. Street, *Phys. Rev. Lett.* **49**, 1187 (1982).
- <sup>32</sup>S. Zafar and E. A. Schiff, *Phys. Rev. Lett.* **66**, 1493 (1991).
- <sup>33</sup>K. Tanaka, *J. Non-Cryst. Solids* **137-138**, 1 (1991).
- <sup>34</sup>S. Yamasaki and J. Isoya, *J. Non-Cryst. Solids* **164-166**, 169 (1993).
- <sup>35</sup>M. Stutzmann, W. B. Jackson, and C. C. Tsai, *Phys. Rev. B* **32**, 23 (1985).
- <sup>36</sup>H. Yokomichi and K. Morigaki, *Solid State Commun.* **63**, 629 (1987).
- <sup>37</sup>H. Hikita, K. Takeda, Y. Kimura, H. Yokomichi, and K. Morigaki, *J. Non-Cryst. Solids* **164-166**, 219 (1993).
- <sup>38</sup>G. Schumm, *Phys. Rev. B* **49**, 2427 (1994).
- <sup>39</sup>J. M. Asensi and J. Andreu, *Phys. Rev. B* **47**, 13 295 (1993).
- <sup>40</sup>S. B. Zhang, W. B. Jackson, and D. J. Chadi, *Phys. Rev. Lett.* **20**, 2575 (1990).